

Subglacial melt channels and fracture in the floating part of Pine Island Glacier, Antarctica

David G. Vaughan,¹ Hugh F. J. Corr,¹ Robert A. Bindschadler,² Pierre Dutrieux,¹ G. Hilmar Gudmundsson,¹ Adrian Jenkins,¹ Thomas Newman,^{3,4} Patricia Vornberger,⁵ and Duncan J. Wingham³

Received 30 January 2012; revised 14 June 2012; accepted 22 June 2012; published 3 August 2012.

[1] A dense grid of ice-penetrating radar sections acquired over Pine Island Glacier, West Antarctica has revealed a network of sinuous subglacial channels, typically 500 m to 3 km wide, and up to 200 m high, in the ice-shelf base. These subglacial channels develop while the ice is floating and result from melting at the base of the ice shelf. Above the apex of most channels, the radar shows isolated reflections from within the ice shelf. Comparison of the radar data with acoustic data obtained using an autonomous submersible, confirms that these echoes arise from open basal crevasses 50–100 m wide aligned with the subglacial channels and penetrating up to 1/3 of the ice thickness. Analogous sets of surface crevasses appear on the ridges between the basal channels. We suggest that both sets of crevasses were formed during the melting of the subglacial channels as a response to vertical flexing of the ice shelf toward the hydrostatic condition. Finite element modeling of stresses produced after the formation of idealized basal channels indicates that the stresses generated have the correct pattern and, if the channels were formed sufficiently rapidly, would have sufficient magnitude to explain the formation of the observed basal and surface crevasse sets. We conclude that ice-shelf basal melting plays a role in determining patterns of surface and basal crevassing. Increased delivery of warm ocean water into the sub-ice shelf cavity may therefore cause not only thinning but also structural weakening of the ice shelf, perhaps, as a prelude to eventual collapse.

Citation: Vaughan, D. G., H. F. J. Corr, R. A. Bindschadler, P. Dutrieux, G. H. Gudmundsson, A. Jenkins, T. Newman, P. Vornberger, and D. J. Wingham (2012), Subglacial melt channels and fracture in the floating part of Pine Island Glacier, Antarctica, *J. Geophys. Res.*, 117, F03012, doi:10.1029/2012JF002360.

1. Introduction

[2] It is increasingly clear that the majority of the current ice loss from the grounded Antarctic ice sheet is a consequence of thinning of ice shelves [Pritchard *et al.*, 2012]. It appears that thinning reduces the restraint an ice shelf exerts on the inland ice, and allows the thinning to be transmitted

inland [Goldberg *et al.*, 2009; Joughin *et al.*, 2010; Payne *et al.*, 2004; Pritchard *et al.*, 2009]. The ice shelf into which Pine Island Glacier, West Antarctica, flows has been thinning for several decades [Bindschadler, 2002; Jenkins *et al.*, 2010] and is now experiencing basal melt at a greater rate than previously [Jacobs *et al.*, 2011]. Although access to the floating ice is hampered by considerable surface crevassing, there is good evidence that considerable melt occurs at ice-shelf base, both from remote sensing [Bindschadler *et al.*, 2011] and from modeling of the ocean circulation [Payne *et al.*, 2007; Thoma *et al.*, 2008]. Similarly, while the extent of the ice shelf remained relatively unchanged for several decades [Vaughan *et al.*, 2001], there is some evidence that a recent ice-front calving has penetrated further into the ice shelf than has been seen previously [Howat *et al.*, 2012].

[3] Upstream of the grounding line, Pine Island Glacier has accelerated [Joughin *et al.*, 2003; Scott *et al.*, 2009] and thinned for years [Wingham *et al.*, 2009]. Recently, the transmission of thinning up the glacier appears to be due to an increase in driving stress, but its future is less certain, with some models suggesting only modest ice loss [Joughin

¹British Antarctic Survey, Natural Environment Research Council, Cambridge, UK.

²NASA and University of Maryland Baltimore County, NASA Goddard Space Flight Center, Greenbelt, Maryland, USA.

³CPOM, Department of Earth Sciences, University College London, London, UK.

⁴Now at NOAA and Earth System Science Interdisciplinary Center, University of Maryland, Silver Spring, Maryland, USA.

⁵Science Applications International Corporation, Beltsville, Maryland, USA.

Corresponding author: D. G. Vaughan, British Antarctic Survey, Natural Environment Research Council, Madingley Road, Cambridge CB3 0ET, UK. (d.vaughan@bas.ac.uk)

©2012. American Geophysical Union. All Rights Reserved. 0148-0227/12/2012JF002360

et al., 2010], while others indicate that rapid grounding-line retreat is possible [Katz and Worster, 2010].

[4] Together, these factors make Pine Island Glacier a valuable natural laboratory in which to study the interaction of ice-shelves and the glaciers that feed them with a changing ocean environment. However, its remote location, pervasive crevassing, rapid flow, and high rates of change mean that Pine Island Glacier is a difficult environment in which to gather informative data sets. In particular, data acquired over multiyear time periods are difficult to interpret because, between measurements, individual features are advected substantial distances and are noticeably deformed by ice flow [Bindschadler *et al.*, 2011].

[5] In support of a planned drilling campaign, a detailed grid of ice-penetrating radar was acquired during a single airborne sortie in January 2011 over a section of the floating part of Pine Island Glacier. The grid was designed to assist in the selection of drill-sites, but the high density of lines, acquired during a single flight, provides a snapshot of unprecedented clarity of the structure of the ice shelf. In this study, we present these radar data and compare them with similar data acquired previously, explore what they imply for ice-ocean interactions, and suggest a specific mechanism that may lead to formation of basal and surface crevasses and weakening of the ice shelf in response to basal melting.

[6] This study follows from similar ground-based and airborne radar surveys of ice shelves in which basal crevasses [Humbert and Steinhage, 2011; Jezek and Bentley, 1983; Luckman *et al.*, 2012; McGrath *et al.*, 2012; Orheim, 1982; Peters *et al.*, 2007; Swithinbank, 1977] and subglacial melt channels [Rignot and Steffen, 2008] have been identified. Several of these studies have addressed the issue of the formation of basal crevasses, emphasizing in particular the maximum height to which they can grow within an ice shelf [Humbert and Steinhage, 2011; Jezek, 1984; van der Veen, 1998; Weertman, 1980]. Here, we combine direct observations with remotely sensed data to build on this research, both revealing the three-dimensional structure of melt channels and basal crevasses and investigating the relationships between them beneath the floating part of Pine Island Glacier. We also integrate these data with a numerical model of ice flexure to focus specifically on crevasse initiation in response to hydrostatic forces that arise from the melting of subglacial channels.

2. Acquisition of Radar Data

[7] Figure 1 shows some of the ice-penetrating radar data used in this study. These data were acquired using the same 150-MHz synthesized pulse system mounted on a Twin-Otter aircraft during two separate field-campaigns; the first, completed in 2004/05, is described elsewhere [Bindschadler *et al.*, 2011; Vaughan *et al.*, 2006], but the second, a dense grid completed during a single flight (Flight C37) on 13th of January 2011, is presented here for the first time.

[8] The 2011 data were acquired on a grid comprising 30 transverse lines across the glacier, each around 20 km long, and with a spacing of roughly 500 m between the lines. The orientation of the lines was selected to be perpendicular to the surface features visible in satellite images in the central part of the ice shelf (Figure 2a). Elevation of the ice-surface

directly beneath the aircraft was simultaneously measured using a nadir-pointing laser altimeter.

[9] Two tie-lines intersecting the transverse lines were also acquired. However, these lines were flown roughly parallel to the major features, and as a result are dominated by off-nadir echoes, which proved difficult to interpret – they are not discussed here.

[10] A variety of synthetic aperture radar (SAR) techniques have been developed to focus, de-clutter and remove off-nadir reflections from airborne radar data [e.g., Hélière *et al.*, 2007; Peters *et al.*, 2005]. We have used a specific technique which is described in detail elsewhere [Newman, 2011]. This method is most effective in collapsing hyperbolae arising from reflectors that are either points directly beneath, or near-horizontal linear features perpendicular to, the flight-track.

3. Results of Radar Survey

[11] Together the two radar data sets (2011 and 2004/05) show the Pine Island Glacier ice shelf to have complex upper and lower surfaces (Figure 1). In the vicinity of the 2004/05 grounding line, the transverse sections (X8 and X7, Figure 1) show ice ~1600-m thick, with only modest variations in the ice-bottom topography. Especially for the fully grounded section, X8, the strength of the ice-bottom reflection is low due to the relatively poor reflectivity of the ice-bed interface. Downstream of X7, substantial features develop in the ice-bottom topography, these features have been discussed in detail elsewhere [Bindschadler *et al.*, 2011], and appear to be transverse to ice-flow (X6 and X5). Further downstream, between sections X4 and X1, a series of subglacial channels develop, which are approximately parallel to ice-flow. The development of these features coincides with substantial thinning of the ice shelf resulting from a combination of longitudinal strain and basal melt [Bindschadler *et al.*, 2011]. The subglacial channels persist downstream into the area covered by the 2011 survey where their structure can be determined with much greater clarity. It is these features that are discussed in detail below.

[12] Sections X3–X1, from the 2004/05 data set, and section X0, which is typical of the 30 sections collected in 2011, all show a similar pattern of features in the ice and in the ice-bottom topography (Figure 1). An echo from the surface of the ice is clearly visible, together with a strong ice-bottom echo. In most areas, a multiple echo from the ice-bottom is also visible; this is typical of the ice-ocean interface and indicates a specular reflection from relatively flat ice-ocean interface. Within each radar section, the basal topography is undulating, with cavities typically 500 m–3 km wide and up to 200 m high in the base of the ice.

[13] When the surface and ice-bottom elevation data from the sections are gridded, the topography of the ice shelf can be seen in great detail (Figures 2b and 2c). In particular, cavities in the ice-bottom can be seen as a series of channels. Over the central section (approximately one third of the grid) these channels roughly follow the direction of ice flow, although they are sinuous, especially in the upstream area. Outside this central section the channels appear to splay outward from the centerline in the downstream direction.

[14] Although a surface expression of most of the basal channels is visible in both satellite imagery and the gridded ice-shelf surface topography (Figure 2b), detailed inspection

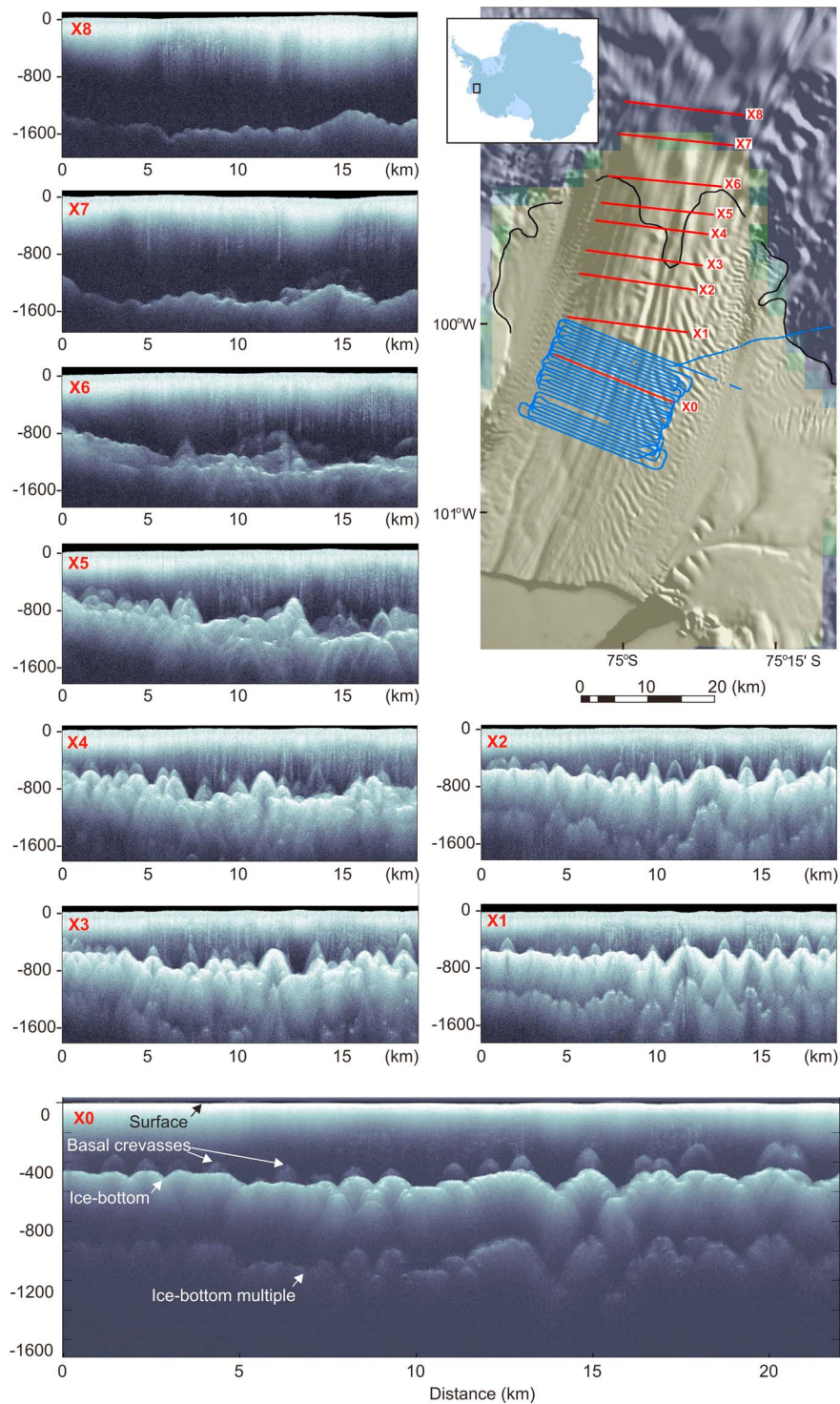


Figure 1. Composite figure showing location of all radar data considered in this study together with representative radar sections X0–X8 (red lines). Location map is based on MODIS image mosaic of Antarctica [Haran *et al.*, 2005], with over-printed color showing grounded ice (blue) and floating ice (beige) determined from a hydrostatic analysis of all radar data collected in 2004/05 [Holt *et al.*, 2006; Vaughan *et al.*, 2006], and 2000 grounding line (dark blue line) determined from InSAR flexing analysis [Rignot, 2002]. Location of radar sections X0 (downstream) acquired in January 2011 and X1 to X8 (upstream) acquired in 2004/05 are shown in red. Location of the other lines acquired in 2011 are shown in blue. Other plots show vertical radar sections (X0–X8) plotted looking upstream with vertical scale in meters and horizontal scale in km. Sections X1–X8, were processed using a focused SAR scheme [Newman, 2011], Section X0 is unprocessed to allow examination of crevasse hyperbolae.

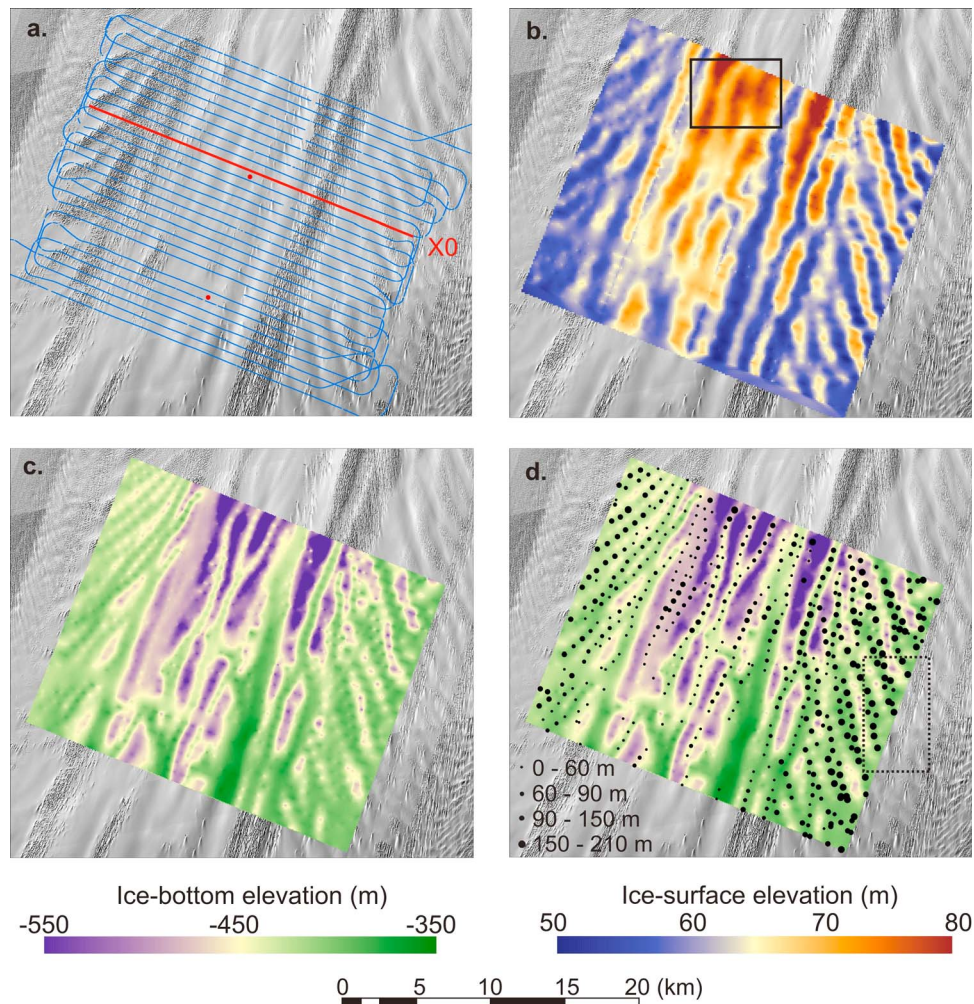


Figure 2. (a) 2011 Flight-tracks, including X0 shown in Figure 1. (b) Grid of surface elevation derived from the laser altimeter with frame showing the extent of Figure 4 (black box). Surface data are reduced to the Eigen-GL04C geoid [Förste *et al.*, 2008] (c) Grid of basal elevation (surface elevation minus ice thickness, calculated assuming no firm correction). (d) Same as c, but also showing locations of basal crevasse tips (black dots) and with frame showing the extent of Figure 3 (dotted black box). Size of dots indicates the height of the crevasse-tip above the surrounding ice bottom. For Figures 2b–2d continuous fields were interpolated using an inverse distance weighting algorithm. In the background are Quickbird images acquired, November 2010, with sun illumination from the right-handed side of the frame.

shows that the surface topography is not a simple inverse of the basal topography, but deviates from perfect local hydrostatic equilibrium as have been noted in many other locations [e.g., Doake *et al.*, 1987; Jenkins, 1990]. Thus, even though the surface elevation data is of high-quality, inversion of it to derive the ice-thickness would, in this case, not reveal the narrow and sinuous nature of the subglacial channels. This discrepancy between surface elevation and ice thickness are likely to be the product of residual bridging stresses sustained in the ice, perhaps density differences due to the presence of crevasses, and possibly englacial debris of the type seen elsewhere on Pine Island Glacier [Corr and Vaughan, 2008].

[15] The sinuosity of the basal channels in the area covered by the 2004/05 survey, the fact that the surface expression of the features is generally wider than their basal expression (compare, Figures 2b and 2c), and the absence of

similar basal channels in the upstream sections (X6, X7, X8), suggests that these channels arise from the melting of the underside of the ice shelf by the ocean beneath. It is not, however, possible to determine whether this melting is constant, or has seasonal or episodic modulation. From our data alone, we cannot draw conclusions about the role that small-scale topography inherited from the grounded ice (c.f. C. V. Gladish *et al.*, Ice shelf basal channels in a coupled ice-ocean model, submitted to *Journal of Glaciology*, 2012), or the pattern of shear in the ice shelf, takes in forming or shaping the specific pattern of channels visible in Figures 2c and 2d. However, the periodicity in ice thickness variations has previously been linked to the periodic influx of ocean water into the sub-shelf cavity thickness variations [Bindshadler *et al.*, 2011], and our data do not appear to contradict that interpretation.

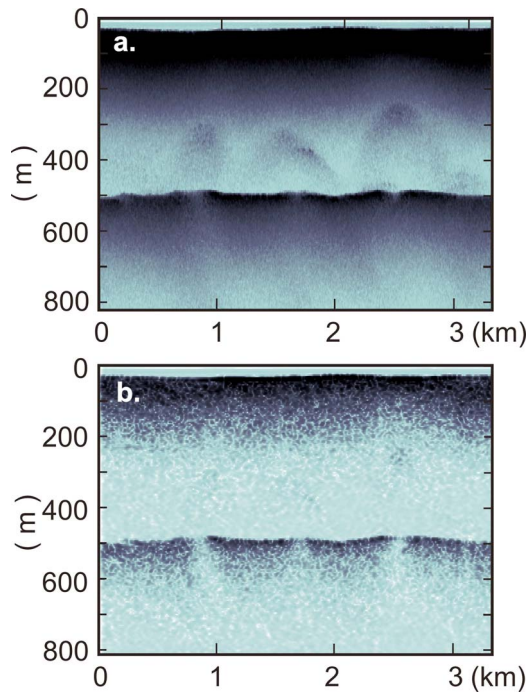


Figure 3. Examples of hyperbolae in the 2011 data, in (a) the raw radar data and (b) the SAR focused data. The SAR processing collapses the hyperbolae indicating that the hyperbolae arise from a point source, or linear feature perpendicular to the flight track.

[16] Similar subglacial channels have been observed on Petermann Glacier, Greenland [Rignot and Steffen, 2008] where they were identified conclusively as resulting from marine melt (Gladish et al., submitted manuscript, 2012). Compared with those on Peterman Glacier, the channels on Pine Island Glacier are similar in width and height, but they are more sinuous, and deviate further from the ice-flow direction – possibly a reflection of the wider subglacial cavity beneath Pine Island Glacier.

[17] In addition to the near continuous ice-bottom echo, on sections X4–X1 and all the 2011 sections, many hyperbolae were also visible within the ice. Use of SAR focusing techniques [Newman, 2011] applied to the along-track data collapsed these hyperbolae effectively to point sources; a strong indication these features arise, either from point features directly beneath the aircraft track or, more likely, from linear features roughly perpendicular to the flight-track (Figure 3). In many cases the ice-bottom reflection beneath the center of the hyperbolae appears to be considerably weaker than on either side. By comparison with those features and similar ones elsewhere [e.g., Luckman et al., 2012; McGrath et al., 2012; Orheim, 1982; Shabtaie and Bentley, 1982] we interpret the hyperbolae in our data as arising from basal crevasses at the ice shelf base. These crevasses appear to penetrate up to 200 m into the ice shelf. Plotting the positions of the tops of the hyperbolae shows that they generally occur above the apex points of the channels in the ice shelf base (Figure 2d). Furthermore the narrow-spacing of the flight lines means we can be confident that the crevasses are relatively continuous along the channels. Neither the unprocessed, nor the SAR-focused, radar data, however, allow us to determine the width of the

crevasses where they intersect the ice-shelf bottom, or indeed whether they are open at the base or filled with marine ice. These questions, can however be addressed through an alternative view of the ice-shelf base presented below.

4. Acoustic Imaging of Basal Crevasses

[18] Acoustic swath mapping of the underside of Pine Island Glacier acquired by an autonomous underwater vehicle, Autosub-3 [Jenkins et al., 2010], was achieved in January 2009. Two Autosub-3 tracks (m429 and m430) overlapped the geographical area covered by the 2011 radar survey, and showed basal crevasses, but these were not imaged well because the trajectory of the vehicle was almost parallel to the crevasses. Another Autosub-3 track obtained during the same campaign (m428, Figure 4) covered an area immediately adjacent to that covered by the 2011 radar survey, and quite clearly imaged a series of basal crevasses trending in roughly the same direction as those identified in the adjacent radar data. Although, the rapid ice-shelf movement of around 4 km per year [Joughin et al., 2010], and observed rates of change in this area means that it is not possible to identify the same basal crevasses in both data sets (collected 2 years apart), the similarity in spatial frequency, direction of trend and location in relation to the subglacial channels strongly suggests that these are identical structures to the basal crevasses observed in the radar data.

[19] The Autosub-3 data show crevasses open at their base and with widths at the base of the ice shelf in the range 50–100 m. Given the narrow geometry of the crevasse and the specification of the swath system on Autosub-3, it is unlikely that the acoustic system would have obtained a reflection from the crevasse apex, and so the actual height of the crevasse was almost certainly greater than the 20–30 m imaged in the acoustic data (Figure 4). Indeed, they could have heights similar to those crevasses seen in the neighboring radar data (~200 m). We currently have no evidence to confirm that the crevasses are open to their tips, and it remains a possibility that some portion of the crevasses contains accreted or unconsolidated marine ice [c.f. Khazendar and Jenkins, 2003].

[20] In summary, the complementary radar and acoustic surveys of Pine Island Glacier indicate that basal melting causes substantial channels to develop in the base of the ice shelf. Associated with these channels, usually above the apex of the channels, there exist narrow basal crevasses. The bottom of these crevasses are open and have widths of 50–100 m, and the crevasses penetrate upwards with vertical heights of up to 210 m – around one third of the total ice-shelf thickness. The surface topography of the ice shelf above the channels generally exhibits the expression expected from hydrostatic relaxation, although residual bridging stresses, or some other factor, may account for deviation from perfect hydrostatic compensation.

5. Surface Crevasses

[21] The surface of the floating part of Pine Island Glacier is highly crevassed and to aid the selection of appropriate drilling sites, high-resolution visible satellite imagery was analyzed to determine the general distribution of crevasses. This analysis showed that while there are several areas of

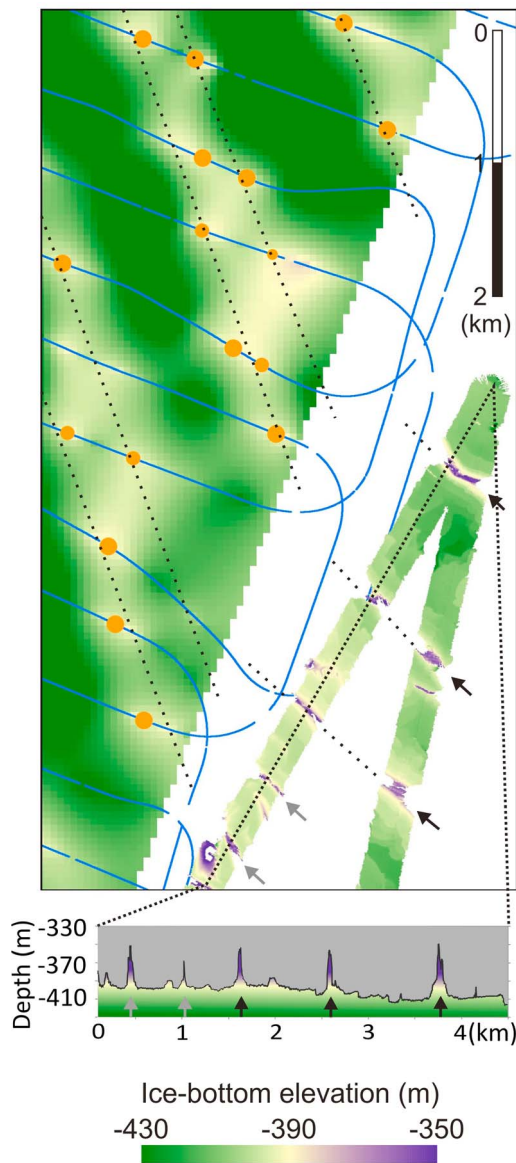


Figure 4. Comparison of the gridded ice-bottom topography derived from the 2011 radar (top left, as in Figure 2) and the ~ 400 -m wide swath acquired in January 2009 by the Autosub-3 acoustic sounder (bottom right), both plotted using the same color-scale. Overlaid on the radar grid are location of flight-tracks (blue lines), apices of basal crevasses (orange dots), and possible locus of basal crevasse tips (dotted lines). A vertical section showing the along-track detail acquired by Autosub-3 along the dotted line is also shown.

rather chaotic crevassing (Figure 5), there are also more subtle bands of crevasses lying along the longitudinal ridges that occupy the central part of the ice shelf. These crevasses appear to align roughly with ice-flow indicating some stress transverse to ice flow. On many ice shelves it would be possible to invoke a higher rate of snow accumulation in the troughs [e.g., Vaughan *et al.*, 2004], allowing more effective burial of the crevasses, but there are several reports [Kellogg *et al.*, 1985] that snow accumulation on the floating part of

Pine Island Glacier is low due to persistent katabatic winds, and for this reason this explanation was considered unsatisfactory. It seems more likely that the appearance of crevasses in specific bands relates to the stresses that caused them.

[22] The process of formation of the subglacial channels by marine melting has been discussed with respect to Petermann Glacier [Rignot and Steffen, 2008; Gladish *et al.*, submitted manuscript, 2012] but the identification of such widespread and significant patterns of basal and surface crevasses does have significant additional implications. In the following sections, we explore processes underlying the formation of these features, and discuss their implications.

6. Hypothesis Regarding Surface and Basal Crevasse Formation

[23] A conceptual model based on the theory of flexure of a linear-elastic thin beam which has been widely and successfully applied to ice shelves [e.g., Holdsworth, 1969; Vaughan, 1995] provides a hypothesis for formation of linear basal crevasses above the subglacial channels beneath the floating part of Pine Island Glacier and the complementary surface crevasses on the ridges between these channels. This allows us to visualize the stresses generated as ocean melting removes ice in the channels at the bottom of the ice shelf (Figure 6). The sagging of the ice surface above the channel toward hydrostatic compensation implies longitudinal compression in the near-surface layers, and corresponding extension in the basal layers. Between channels, and perhaps on the margins of isolated channels, the opposite effect should be seen: extension in the surface layers and compression in the basal layers.

[24] The location and orientation of longitudinal surface crevasses along the surface ridges, and basal crevasses

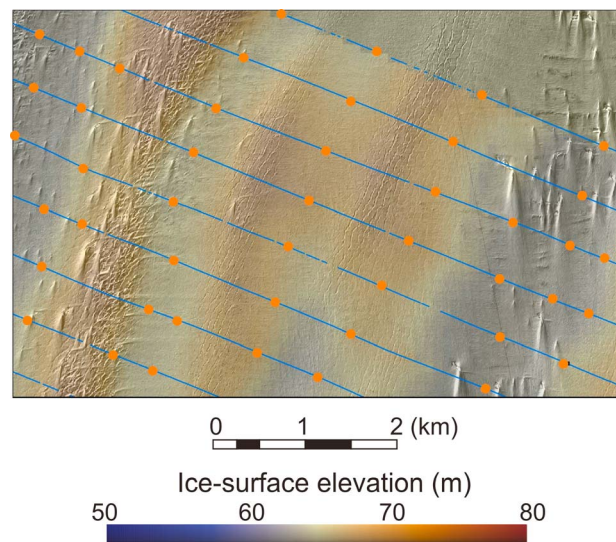


Figure 5. Flight-tracks (blue lines) and locations of basal crevasse-tips (orange dots) overlaid on Quickbird imagery acquired on January 16, 2011, sub-sampled to 5-m resolution, and tinted with color indicating derived surface elevation (as in Figure 2b). The extent of the frame is shown in Figure 2b.

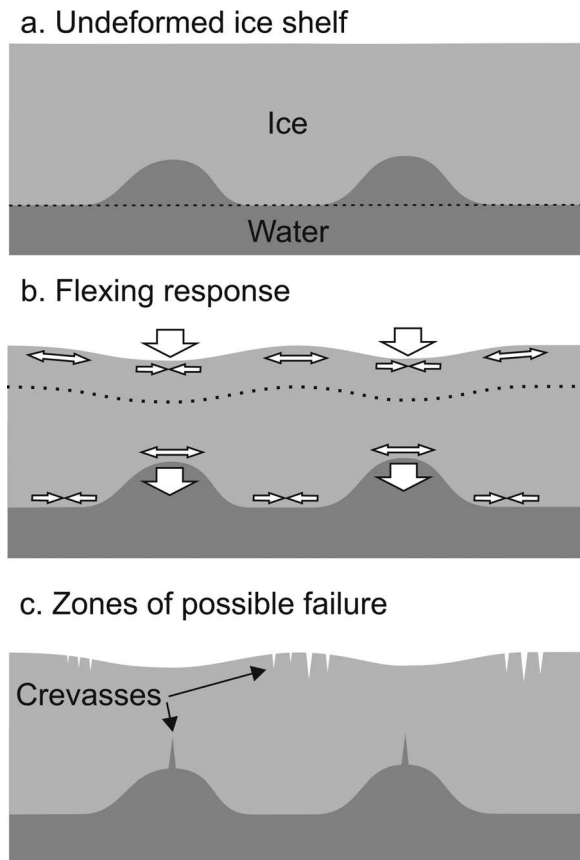


Figure 6. Drawing of the formation of surface and basal crevasses based on thin-beam theory.

roughly above the apex of the channels could thus be explained by transverse extensional stresses predicted by this model. However, the thin-beam analysis cannot be used in a quantitative sense to predict the pattern or magnitude of stresses because the underlying assumptions are not properly satisfied: 1. the widths of the basal channels are narrow compared with the thickness of the ice shelf, and their vertical dimensions are a considerable fraction of the total ice thickness; 2. The ice is not expected to deform in a purely linear-elastic manner, but should be approximated by a nonlinear viscous rheology; 3. The effect of temperature variations on the viscosity of the ice ought not to be ignored. For these reasons, we have sought to test the hypotheses generated by our thin-beam model using a less intuitive approach, of finite element modeling.

7. Finite Element Model

[25] In order to test our hypothesis regarding formation of basal and surface crevasses, we have used a finite element (FE) model to determine the maximum stresses generated in a 2-dimensional vertical section of an idealized ice shelf after the instantaneous formation of two basal channels with dimensions similar to those observed beneath Pine Island Glacier. The approach is a development of linear viscous FE models used widely elsewhere; for example, to determine the longevity of flow stripes on an ice shelf [Casassa and

Whillans, 1994] and for vertical glaciers walls [Hanson and Hooke, 2003]. The approach has allowed us to verify whether the pattern of stresses in the ice is similar to that suggested by the conceptual model, and that those stresses are of the correct order of magnitude to cause the ice to fracture.

[26] We undertook the FE modeling using Marc/Mentat finite element software (Version 2010.1.0 64-bit). The basic geometry comprised a 727-m thick shelf that begins with a completely flat surface and a horizontal extent of 20.5 km. From the surface to sea level the temperature is set to -20°C , below this, temperature increases linearly to 0°C at the ice-bottom. The ice rheology is represented using a standard Glen flow law ($n = 3$), with temperature dependency taken from [Smith and Morland, 1981]. From this slab, two channels, 1.6 km wide and 200 m high (identical in shape to the one at km 15 in X0, Figure 1), were excavated from the base of the ice shelf with their peaks 4.4 km apart. The ice-shelf was divided into a domain of 8-node quadrilateral elements using bi-quadratic interpolation functions, each of which was $1/12$ of the full ice thickness and 100 m wide.

[27] From the start of the simulation, the ice shelf was allowed to adjust to the hydrostatic imbalance introduced by the presence of the channels, assuming stresses imposed an ice density of 900 kg m^{-3} , and water density of 1030 kg m^{-3} . The weight of the ice was applied separately to each element, and this was opposed by a variable ocean pressure applied normally to the lower edges of the basal elements. The horizontal margins for the domain were allowed to move only vertically maintaining the initial width of the ice shelf. Using a slightly different geometry (describing an ice cliff) the function of the model was verified by comparison with stress solutions presented elsewhere [Hanson and Hooke, 2003, Figure 1c].

[28] The results of the model simulation are summarized by the pattern of deviatoric stresses shown in Figure 7. Figure 7 (top) shows the stresses 0.5 days after the instantaneous excavation of the basal channels. At this point, the tendency for the ice over the channels to sag toward the hydrostatic level generates horizontal compressive stresses of $>600\text{ kPa}$ at the surface and extensive deviatoric stresses in excess of $\sim 300\text{ kPa}$ at the ice base just above the apex of the channel. As sagging proceeds (Figure 7, bottom), extensive horizontal stresses grow on the surface between the channels, eventually exceeding 300 kPa , with a reduction in the extensive stresses in the basal ice. If the model is allowed to evolve in time, eventually, the flow of the ice shelf toward the relaxed state of hydrostatic compensation allows the stresses to dissipate.

[29] Although it is difficult to be precise, the magnitude of the deviatoric stresses suggested by the model is probably sufficient to fracture basal and surface layers of the ice. Earlier studies have suggested that crevassing was likely to be produced in surface layers when regional stresses exceed $90\text{--}320\text{ kPa}$ [Vaughan, 1993]. There is, however, very little literature to allow us to establish whether basal crevasses are likely to be formed at similar stresses, but since instantaneous failure of full-density ice is expected at stresses of around 1 MPa , it does not seem implausible that sustained stresses of this magnitude would cause basal crevasses.

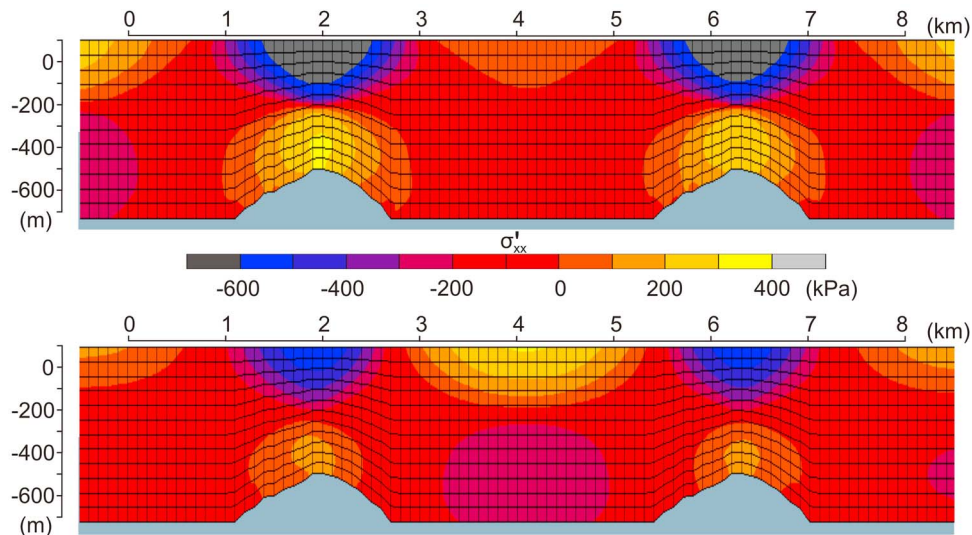


Figure 7. Subset of the finite element modeling domain showing longitudinal deviatoric stresses (σ'_{xx}) generated immediately (top) after excavation of subglacial channels and (bottom) after relaxation to the hydrostatic. Black lines show the finite elements boundaries. Vertical coordinate measured from sea level. Areas of maximum extensive stress are visible in Figure 7 (top) in the basal ice directly above the apex of each subglacial channel, and in Figure 7 (bottom) on the surface between the channels.

[30] Interestingly, the simulation indicates that there is no identifiable continuous neutral surface (the notional surface corresponding to zero horizontal deviatoric stress) in the ice shelf. This, in itself, confirms that the thin-beam approximation could not be used to predict the detailed pattern or magnitude of the induced stresses, and that the finite element approach is required.

[31] Furthermore, the effect of applying a temperature variation to the ice viscosity appears to have little impact on the magnitude of the extensive stresses either at the surface or the base, nor compressive stresses near the base. However, it does substantially increase the magnitude of the compressive stresses generated near the ice surface.

[32] The finite element approach described above is valuable, but still leaves some open questions that could only be addressed by a more complete sensitivity study. The instantaneous excavation of the ice-bottom channels allows the maximum stresses in the basal ice to be realized, but generating these stresses requires that channels must be created rapidly compared with the time taken for the relaxation of the hydrostatic imbalance. If melting and relaxation occur on a similar timescale then rather lower stresses would be generated. Although such an approach may be possible, the time-evolution of our finite element model and the resultant stress-field is not sufficiently well verified against known solutions that we are confident to use it to constrain the rates of melting required to produce the basal or surface crevasses. It is also likely that surface crevassing will be generated most readily by melting of channels that are optimally separated: if the channels are too far apart, their stress fields will not interact, and if they are too close together the ice will tend to sag as if it were responding to a single load, without producing the bending required to create deviatoric stresses in the near-surface layers. Similarly, a

simulation that captures the evolution of stress during the fracture process would require application of a specific failure criterion that included dependency on temperature and confining-pressure, for which there is little basis in the published literature.

8. Conclusions

[33] Our analysis of satellite imagery and airborne radar data suggest that there are significant channels in the base of Pine Island Glacier, which are formed through the melting action of the ocean on the ice. These channels are expressed, in an attenuated form, in the surface morphology of the ice shelf. The origin of the complex morphology of the channels is at present unclear, but it appears to be the result of oceanographic currents and is similar to those predicted by recent oceanographic modeling (Gladish et al., submitted manuscript, 2012). Associated with the channels are swarms of surface crevasses and individual basal crevasses that appear to form during the hydrostatic relaxation of the ice shelf in response to the formation of the ice-bottom channels. The basal crevasses are narrow (50–100 m) and open to the ocean at the ice-shelf base but extend up to 200 m into the ice shelf.

[34] Similar subglacial melt channels were reported on Petermann Glacier in Greenland, but despite the use of comparable radar, associated basal crevasses were not reported in that case [Rignot and Steffen, 2008]. Similarly, there are many reports of basal crevasses in ice shelves around Antarctica [Humbert and Steinhage, 2011; Jezek and Bentley, 1983; Luckman et al., 2012; McGrath et al., 2012; Orheim, 1982; Peters et al., 2007; Swithinbank, 1977]. In two of these, there was evidence of surface crevasses in roughly the same configuration to the basal crevasses that

we have identified [Luckman *et al.*, 2012; McGrath *et al.*, 2012], one of these identified hydrostatic relaxation in response to basal crevasse as the likely sources of surface crevasses. Our observations allow us to identify basal melt as the cause of basal and surface crevassing on Pine Island Glacier, with hydrostatic relaxation transferring vertical stresses to horizontal ones. Finally, an opposite effect, where freezing of marine ice beneath an ice shelf causes hydrostatic uplift and zones of chaotic surface crevassing has also been reported [Thyssen *et al.*, 1993].

[35] Taken together, the studies discussed above indicate a growing body of evidence that localized mass changes at the base of ice shelves (melt and freeze-on) have widespread significance to the distribution of fracture (surface and basal) in ice shelves. It was already evident that increasing the supply of warm water beneath an ice shelf could thin and weaken the ice shelf by increasing the rate of basal melting, and that the impact of melt could be enhanced along narrow channels [Rignot and Steffen, 2008], but it is now also apparent that formation of basal crevasses and surface crevasses in response to melt channel formation could exacerbate this weakening. While the mechanism proposed could not cause full-thickness rifting, if basal melting of ice shelves in warm oceanographic environments plays a role, not only in controlling the mass balance of the ice shelf, but also in promoting surface and basal fracture it could nonetheless decrease the overall integrity of the ice shelf.

[36] To date, most of the processes that have been suggested as responsible for the retreat and eventual collapse of several ice shelves along the Antarctic Peninsula have involved production of surface meltwater rather than any oceanic influence [Doake and Vaughan, 1991; MacAyeal *et al.*, 2003; Scambos *et al.*, 2003, 2009]. This interpretation is supported by the pattern of ice-shelf retreat along the Antarctic Peninsula that closely matched the pattern of surface temperature and the abundance of summer melting [Morris and Vaughan, 2003]. However, current mean annual air temperatures over the ice shelves of Amundsen Sea sector of West Antarctica, and over the Ross and Ronne-Filchner ice shelves, are substantially below that required for any significant quantities surface melt, and so none of these ice shelves is considered to be under any imminent threat from atmospheric warming. If, however, the effect of increasing heat-delivery beneath the ice shelf is to cause increased fracture and loss of structural integrity, then this alone might eventually lead to ice-shelf disintegration before atmospheric temperatures warm sufficiently to generate surface-driven breakup. Indeed, recent oceanographic projections driven by global climate projections suggest that ocean heat delivery to Filchner-Ronne Ice Shelf may substantially increase toward the end of the 21st Century, which would cause melt-rates similar in magnitude to those currently seen on Pine Island Glacier [Hellmer *et al.*, 2012]. This suggests that the processes we have observed to be active beneath Pine Island Glacier may eventually become more widespread.

[37] **Acknowledgments.** We thank colleagues at British Antarctic Survey for constructive advice, and in particular, Carl Robinson and Captain Doug Cochrane, who acquired the radar data. The work is part of the British Antarctic Survey program, Polar Science for Planet Earth funded in part by the Natural Environment Research Council. DGV was funded by the EU FP7 program ice2sea (grant 226375, pub. no. 076). TN and DJW acknowledge the support of the NERC National Centre for Earth Observation. Autosub-3 data collection and PD were supported by NERC Grant

NE/G001367/1. Radar data acquired for this study are available at <https://secure.antarctica.ac.uk/data/aerogeo/index.php>

References

- Bindschadler, R. A. (2002), History of lower Pine Island Glacier, West Antarctica, from Landsat imagery, *J. Glaciol.*, *48*(163), 536–544, doi:10.3189/172756502781831052.
- Bindschadler, R. A., D. G. Vaughan, and P. Vormberger (2011), Variability of basal melt beneath the Pine Island Glacier ice shelf, West Antarctica, *J. Glaciol.*, *57*(204), 581–595, doi:10.3189/002214311797409802.
- Casassa, G., and I. M. Whillans (1994), Decay of surface topography on the Ross Ice Shelf, Antarctica, *Ann. Glaciol.*, *20*, 249–253, doi:10.3189/172756494794587500.
- Corr, H. F. J., and D. G. Vaughan (2008), A recent volcanic eruption beneath the West Antarctic ice sheet, *Nat. Geosci.*, *1*, 122–125, doi:10.1038/ngeo106.
- Doake, C. S. M., and D. G. Vaughan (1991), Rapid disintegration of Wordie Ice Shelf in response to atmospheric warming, *Nature*, *350*, 328–330, doi:10.1038/350328a0.
- Doake, C. S. M., R. M. Frolich, D. R. Mantripp, A. M. Smith, and D. G. Vaughan (1987), Glaciological studies of Rutford Ice Stream, Antarctica, *J. Geophys. Res.*, *92*(B9), 8951–8960, doi:10.1029/JB092iB09p08951.
- Förste, C., et al. (2008), The GeoForschungsZentrum Potsdam/Groupe de Recherche de Géodésie Spatiale satellite-only and combined gravity field models: EIGEN-GL04S1 and EIGEN-GL04C, *J. Geod.*, *82*(6), 331–346, doi:10.1007/s00190-007-0183-8.
- Goldberg, D., D. M. Holland, and C. Schoof (2009), Grounding line movement and ice shelf buttressing in marine ice sheets, *J. Geophys. Res.*, *114*, F04026, doi:10.1029/2008JF001227.
- Hanson, B., and R. L. Hooke (2003), Buckling rate and overhang development at a calving face, *J. Glaciol.*, *49*(167), 577–586, doi:10.3189/172756503781830476.
- Haran, T., J. Bohlander, T. Scambos, T. Painter, and M. Fahnestock (2005), MODIS mosaic of Antarctica (MOA) image map, <http://nsidc.org/data/nsidc-0280.html>, Natl. Snow and Ice Data Cent., Boulder, Colo.
- Hélière, F., C.-C. Lin, H. Corr, and D. Vaughan (2007), Radio echo sounding of Pine Island Glacier, West Antarctica: Aperture synthesis processing and analysis of feasibility from space, *IEEE Trans. Geosci. Remote Sens.*, *45*(8), 2573–2582, doi:10.1109/TGRS.2007.897433.
- Hellmer, H., F. Kauker, R. Timmermann, J. Determann, and J. Rae (2012), Twenty-first-century warming of a large Antarctic ice-self cavity by a redirected coastal current, *Nature*, *485*, 225–228, doi:10.1038/nature11064.
- Holdsworth, G. (1969), Flexure of a floating ice tongue, *J. Glaciol.*, *8*, 385–397.
- Holt, J. W., D. D. Blankenship, D. L. Morse, D. A. Young, M. E. Peters, S. D. Kempf, T. G. Richter, D. G. Vaughan, and H. F. J. Corr (2006), New boundary conditions for the West Antarctic Ice Sheet: Subglacial topography of the Thwaites and Smith glacier catchments, *Geophys. Res. Lett.*, *33*, L09502, doi:10.1029/2005GL025561.
- Howat, I. M., K. Jezek, M. Studinger, J. A. MacGregor, J. Paden, D. Floricioiu, R. Russell, M. Linkswiler, and R. T. Dominguez (2012), Rift in Antarctic glacier: A unique chance to study ice shelf retreat, *Eos Trans. AGU*, *93*(8), 77, doi:10.1029/2012EO080001.
- Humbert, A., and D. Steinhage (2011), The evolution of the western rift area of the Fimbul Ice Shelf, Antarctica, *Cryosphere*, *5*(4), 931–944, doi:10.5194/tc-5-931-2011.
- Jacobs, S. S., A. Jenkins, C. F. Giulivi, and P. Dutrieux (2011), Stronger ocean circulation and increased melting under Pine Island Glacier ice shelf, *Nat. Geosci.*, *4*(8), 519–523, doi:10.1038/ngeo1188.
- Jenkins, A. (1990), Recent investigations of surface undulations where Rutford Ice Stream enters Ronne Ice Shelf, in *Filchner Ronne Ice Shelf Programme, Rep. 4*, edited by H. Oerter, pp. 12–17, Alfred-Wegener Inst. for Polar and Mar. Res, Bremerhaven, Germany.
- Jenkins, A., P. Dutrieux, S. S. Jacobs, S. D. McPhail, J. R. Perrett, A. T. Webb, and D. White (2010), Observations beneath Pine Island Glacier in West Antarctica and implications for its retreat, *Nat. Geosci.*, *3*(7), 468–472, doi:10.1038/ngeo890.
- Jezek, K. C. (1984), A modified theory of bottom crevasses used as a means for measuring the buttressing effect of ice shelves on inland ice sheets, *J. Geophys. Res.*, *89*(B3), 1925–1931, doi:10.1029/JB089iB03p01925.
- Jezek, K. C., and C. R. Bentley (1983), Field studies of bottom crevasses in the Ross Ice Shelf, Antarctica, *J. Glaciol.*, *29*(101), 118–126.
- Joughin, I., E. Rignot, C. E. Rosanova, B. K. Lucchitta, and J. Bohlander (2003), Timing of recent accelerations of Pine Island Glacier, Antarctica, *Geophys. Res. Lett.*, *30*(13), 1706, doi:10.1029/2003GL017609.
- Joughin, I., B. E. Smith, and D. M. Holland (2010), Sensitivity of 21st century sea level to ocean-induced thinning of Pine Island Glacier, Antarctica, *Geophys. Res. Lett.*, *37*, L20502, doi:10.1029/2010GL044819.

- Katz, R. F., and M. G. Worster (2010), Stability of ice-sheet grounding lines, *Proc. R. Soc. A*, 466(2118), 1597–1620, doi:10.1098/rspa.2009.0434.
- Kellogg, T. B., D. E. Kellogg, and T. J. Hughes (1985), Amundsen Sea sediment coring, *Antarct. J. U. S.*, 20(5), 79–81.
- Khazendar, A., and A. Jenkins (2003), A model of marine ice formation within Antarctic ice shelf rifts, *J. Geophys. Res.*, 108(C7), 3235, doi:10.1029/2002JC001673.
- Luckman, A., D. Jansen, B. Kulesa, E. C. King, P. Sammonds, and D. I. Benn (2012), Basal crevasses in Larsen C Ice Shelf and implications for their global abundance, *Cryosphere*, 6, 113–123, doi:10.5194/tc-6-113-2012.
- MacAyeal, D. R., T. A. Scambos, C. L. Hulbe, and M. A. Fahnestock (2003), Catastrophic ice-shelf break-up by an ice-shelf-fragment-capsize mechanism, *J. Glaciol.*, 49(164), 22–36, doi:10.3189/172756503781830863.
- McGrath, D., K. Steffen, T. Scambos, H. Rajaram, G. Casassa, and J. L. Rodriguez Lagos (2012), Basal crevasses and associated surface crevassing on the Larsen C Ice Shelf, Antarctica and their role in ice-shelf instability, *Ann. Glaciol.*, 53(60), 10–18, doi:10.3189/2012AoG60A005.
- Morris, E. M., and D. G. Vaughan (2003), Spatial and temporal variation of surface temperature on the Antarctic Peninsula and the limit of viability of ice shelves, in *Antarctic Peninsula Climate Variability: Historical and Paleoenvironmental Perspectives*, *Antarct. Res. Ser.*, vol. 79, edited by E. Domack et al., pp. 61–68, AGU, Washington, D. C., doi:10.1029/AR079p0061.
- Newman, T. (2011), Application of synthetic aperture techniques to radar echo soundings of the Pine Island Glacier, Antarctica, PhD thesis, Univ. Coll. London, London.
- Orheim, O. (1982), Radio echo-sounding of Riiser-Larsenisen, *Ann. Glaciol.*, 3, 355.
- Payne, A. J., A. Vieli, A. P. Shepherd, D. J. Wingham, and E. Rignot (2004), Recent dramatic thinning of largest West Antarctic ice stream triggered by oceans, *Geophys. Res. Lett.*, 31, L23401, doi:10.1029/2004GL021284.
- Payne, A. J., P. R. Holland, A. P. Shepherd, I. C. Rutt, A. Jenkins, and I. Joughin (2007), Numerical modeling of ocean-ice interactions under Pine Island Bay's ice shelf, *J. Geophys. Res.*, 112, C10019, doi:10.1029/2006JC003733.
- Peters, M. E., D. D. Blankenship, and D. L. Morse (2005), Analysis techniques for coherent airborne radar sounding: Application to West Antarctic ice streams, *J. Geophys. Res.*, 110, B06303, doi:10.1029/2004JB003222.
- Peters, M. E., D. D. Blankenship, D. E. Smith, J. W. Holt, and S. D. Kempf (2007), The distribution and classification of bottom crevasses from radar sounding of a large tabular iceberg, *IEEE Geosci. Remote Sens. Lett.*, 4(1), 142–146, doi:10.1109/LGRS.2006.887057.
- Pritchard, H. D., R. J. Arthern, D. G. Vaughan, and L. A. Edwards (2009), Extensive dynamic thinning at the margins of the Greenland and Antarctic ice sheets, *Nature*, 461(7266), 971–975, doi:10.1038/nature08471.
- Pritchard, H. D., S. R. M. Ligtenberg, H. A. Fricker, D. G. Vaughan, M. R. van den Broeke, and L. Padman (2012), Antarctic ice-sheet loss driven by basal melting of ice shelves, *Nature*, 484, 502–505, doi:10.1038/nature10968.
- Rignot, E. (2002), Ice-shelf changes in Pine Island Bay, Antarctica, 1947–2000, *J. Glaciol.*, 48(161), 247–256, doi:10.3189/172756502781831386.
- Rignot, E., and K. Steffen (2008), Channelized bottom melting and stability of floating ice shelves, *Geophys. Res. Lett.*, 35, L02503, doi:10.1029/2007GL031765.
- Scambos, T., C. Hulbe, and M. Fahnestock (2003), Climate-induced ice shelf disintegration in the Antarctic Peninsula, in *Antarctic Peninsula Climate Variability: Historical and Paleoenvironmental Perspectives*, *Antarct. Res. Ser.*, vol. 79, edited by E. Domack et al., pp. 79–92, AGU, Washington, D. C., doi:10.1029/AR079p0079.
- Scambos, T., H. A. Fricker, C.-C. Liu, J. Bohlander, J. Fastook, A. Sargent, R. Massom, and A.-M. Wu (2009), Ice shelf disintegration by plate bending and hydro-fracture: Satellite observations and model results of the 2008 Wilkins ice shelf break-ups, *Earth Planet. Sci. Lett.*, 280(1–4), 51–60, doi:10.1016/j.epsl.2008.12.027.
- Scott, J. B. T., G. H. Gudmundsson, A. M. Smith, R. G. Bingham, H. D. Pritchard, and D. G. Vaughan (2009), Increased rate of acceleration on Pine Island Glacier strongly coupled to changes in gravitational driving stress, *Cryosphere*, 3, 125–131, doi:10.5194/tc-3-125-2009.
- Shabtaie, S., and C. R. Bentley (1982), Tabular icebergs: Implications from geophysical studies of ice shelves, *J. Glaciol.*, 28(100), 413–430.
- Smith, G. D., and L. W. Morland (1981), Viscous relations for the steady creep of polycrystalline ice, *Cold Reg. Sci. Technol.*, 5(2), 141–150, doi:10.1016/0165-232X(81)90048-3.
- Swithinbank, C. (1977), Glaciological research in the Antarctic Peninsula, *Philos. Trans. R. Soc. London B*, 279(963), 161–183, doi:10.1098/rstb.1977.0080.
- Thoma, M., A. Jenkins, D. Holland, and S. Jacobs (2008), Modelling Circumpolar Deep Water intrusions on the Amundsen Sea continental shelf, Antarctica, *Geophys. Res. Lett.*, 35, L18602, doi:10.1029/2008GL034939.
- Thyssen, F., A. Bombosch, and H. Sandhäger (1993), Elevation, ice thickness and structure mark maps of the central part of Filchner-Ronne Ice Shelf, *Polarforschung*, 62, 17–26.
- van der Veen, C. J. (1998), Fracture mechanics approach to penetration of bottom crevasses on glaciers, *Cold Reg. Sci. Technol.*, 27(3), 213–223, doi:10.1016/S0165-232X(98)00006-8.
- Vaughan, D. G. (1993), Relating the occurrence of crevasses to surface strain rates, *J. Glaciol.*, 39, 255–266.
- Vaughan, D. G. (1995), Tidal flexure at ice shelf margins, *J. Geophys. Res.*, 100(B4), 6213–6224, doi:10.1029/94JB02467.
- Vaughan, D. G., A. M. Smith, H. F. J. Corr, A. Jenkins, C. R. Bentley, M. D. Stenoien, S. S. Jacobs, T. B. Kellogg, E. Rignot, and B. K. Lucchitta (2001), A review of Pine Island Glacier, West Antarctica: Hypotheses of instability vs. observations of change, in *The West Antarctic Ice Sheet: Behavior and Environment*, *Antarct. Res. Ser.*, vol. 77, edited by R. B. Alley and R. A. Bindshadler, pp. 237–256, AGU, Washington, D. C., doi:10.1029/AR077p0237.
- Vaughan, D. G., P. S. Anderson, J. C. King, G. W. Mann, S. D. Mobbs, and R. S. Ladkin (2004), Imaging of firn isochrones across an Antarctic ice rise and implications for patterns of snow accumulation rate, *J. Glaciol.*, 50(170), 413–418, doi:10.3189/172756504781829882.
- Vaughan, D. G., H. F. J. Corr, F. Ferraccioli, N. Frearson, A. O'Hare, D. Mach, J. W. Holt, D. D. Blankenship, D. L. Morse, and D. A. Young (2006), New boundary conditions for the West Antarctic ice sheet: Subglacial topography beneath Pine Island Glacier, *Geophys. Res. Lett.*, 33, L09501, doi:10.1029/2005GL025588.
- Weertman, J. (1980), Bottom crevasses, *J. Glaciol.*, 25(91), 185–188.
- Wingham, D. J., D. W. Wallis, and A. Shepherd (2009), Spatial and temporal evolution of Pine Island Glacier thinning, 1995–2006, *Geophys. Res. Lett.*, 36, L17501, doi:10.1029/2009GL039126.